

University of Groningen

Isolation and characterization of a thermostable F420:NADPH oxidoreductase from *Thermobifida fusca*

Kumar, Hemant; Nguyen, Quoc-Thai; Binda, Claudia; Mattevi, Andrea; Fraaije, Marco W

Published in:
The Journal of Biological Chemistry

DOI:
[10.1074/jbc.M117.787754](https://doi.org/10.1074/jbc.M117.787754)

IMPORTANT NOTE: You are advised to consult the publisher's version (publisher's PDF) if you wish to cite from it. Please check the document version below.

Document Version
Publisher's PDF, also known as Version of record

Publication date:
2017

[Link to publication in University of Groningen/UMCG research database](#)

Citation for published version (APA):

Kumar, H., Nguyen, Q-T., Binda, C., Mattevi, A., & Fraaije, M. W. (2017). Isolation and characterization of a thermostable F420:NADPH oxidoreductase from *Thermobifida fusca*. *The Journal of Biological Chemistry*, 292, 10123-10130. [jbc.M117.787754]. <https://doi.org/10.1074/jbc.M117.787754>

Copyright

Other than for strictly personal use, it is not permitted to download or to forward/distribute the text or part of it without the consent of the author(s) and/or copyright holder(s), unless the work is under an open content license (like Creative Commons).

The publication may also be distributed here under the terms of Article 25fa of the Dutch Copyright Act, indicated by the "Taverne" license. More information can be found on the University of Groningen website: <https://www.rug.nl/library/open-access/self-archiving-pure/taverne-amendment>.

Take-down policy

If you believe that this document breaches copyright please contact us providing details, and we will remove access to the work immediately and investigate your claim.

Downloaded from the University of Groningen/UMCG research database (Pure): <http://www.rug.nl/research/portal>. For technical reasons the number of authors shown on this cover page is limited to 10 maximum.

Isolation and characterization of a thermostable F₄₂₀:NADPH oxidoreductase from *Thermobifida fusca*

Hemant Kumar,^{1,#} Quoc-Thai Nguyen,^{1,2,3,#} Claudia Binda,⁴ Andrea Mattevi,⁴
and Marco W. Fraaije¹

¹ Molecular Enzymology Group, Groningen Biomolecular Sciences and Biotechnology Institute, University of Groningen, Nijenborgh 4, 9747 AG Groningen, The Netherlands.

² Scuola Universitaria Superiore IUSS Pavia, Piazza della Vittoria 15, 27100 Pavia, Italy

³ Faculty of Pharmacy, University of Medicine and Pharmacy, Ho Chi Minh City, 41 Dinh Tien Hoang Street, Ben Nghe Ward, District 1, Ho Chi Minh City, Vietnam

⁴ Department of Biology and Biotechnology, University of Pavia, Via Ferrata 1, 27100 Pavia, Italy

These authors contributed equally to this work

To whom correspondence should be addressed: Prof. dr. M.W. Fraaije, Molecular Enzymology Group, Groningen Biomolecular Sciences and Biotechnology Institute, University of Groningen, Nijenborgh 4, 9747 AG Groningen, The Netherlands. Tel: +31503634345. Email: m.w.fraaije@rug.nl.

Keywords: *Thermobifida fusca*, F₄₂₀, deazaflavoenzymes, oxidoreductase, nicotinamide adenine dinucleotide phosphate

Running title: F₄₂₀:NADPH oxidoreductase from *T. fusca*

Abbreviations used: FNO, F₄₂₀:NADPH oxidoreductase; Tfu, *Thermobifida fusca*; Af, *Archaeoglobus fulgidus*; NAD(P)⁺, nicotinamide adenine dinucleotide (phosphate)

Abstract

F₄₂₀H₂-dependent enzymes reduce a wide range of substrates that are otherwise recalcitrant to enzyme-catalyzed reduction, and their potential for applications in biocatalysis has attracted increasingly attention. *Thermobifida fusca* is a moderately thermophilic bacterium and holds high biocatalytic potential as a source for several highly thermostable enzymes. We report here on the isolation and characterization of a thermostable F₄₂₀:NADPH oxidoreductase (Tfu-FNO) from *T. fusca*, being the first F₄₂₀-dependent enzyme described from this bacterium. Tfu-FNO was heterologously expressed in *Escherichia coli*, yielding up to 200 mg recombinant enzyme per liter of culture. We found that Tfu-FNO is highly thermostable, reaching its highest activity at 65 °C and that Tfu-FNO is likely to act *in vivo* as an F₄₂₀ reductase at the expense of NADPH, similar to its counterpart in *Streptomyces griseus*. We obtained the crystal structure of FNO in complex with NADP⁺ at 1.8 Å resolution, providing the first bacterial FNO structure. The overall architecture and NADP⁺-binding site of Tfu-FNO were highly similar to those of the *Archaeoglobus fulgidus* FNO (Af-FNO). The active site is located in a hydrophobic pocket between an N-terminal dinucleotide-binding domain and a smaller C-terminal

domain. Residues interacting with the 2'-phosphate of NADP⁺ were probed by targeted mutagenesis, indicating that Thr28, Ser50, Arg51, and Arg55 are important for discriminating between NADP⁺ and NAD⁺. Interestingly, a T28A mutant increased the kinetic efficiency more than three-fold as compared with the wild-type enzyme when NADH is the substrate. The biochemical and structural data presented here provide crucial insights into the molecular recognition of the two cofactors, F₄₂₀ and NAD(P)H by FNO.

Introduction

Flavins can arguably be regarded as the most extensively studied redox cofactors. One natural flavin analogue is cofactor F₄₂₀ which was first isolated and characterized from methanogenic archaea in 1972 (1). Since then, F₄₂₀ has been found in members of methanogens, actinomycetes, cyanobacteria, and some betaproteobacteria (2). Replacement of the 5' nitrogen of flavins with a carbon in F₄₂₀, resulting in a so-called deazaflavin, renders the cofactor nearly unreactive towards molecular oxygen. Hence, F₄₂₀ is an obligate hydride-transfer cofactor similar to the nicotinamide cofactors (Fig. 1). Besides, the 8'-OH group on the isoalloxazine ring in

F₄₂₀ has been suggested to slow down the autooxidation of the reduced cofactor (F₄₂₀H₂) in air, thus the reduced species is much more stable than that of flavins (3).

Many F₄₂₀(H₂)-dependent enzymes have been characterized recently and their potential for applications in biocatalysis has attracted increasing attention (4,5). F₄₂₀-dependent enzymes studied so far have been shown to be capable of reducing a wide range of substrates which are otherwise recalcitrant to enzyme-catalyzed reduction (4,5). However, the commercial unavailability of cofactor F₄₂₀ remains a bottleneck for studying and applying the respective enzymes. Therefore, it would be attractive to have access to an efficient F₄₂₀H₂ cofactor recycling system. In this context, F₄₂₀:NADPH oxidoreductases (FNOs, E.C. 1.5.1.40, Fig. 1) could become very valuable as NADPH-driven F₄₂₀H₂-recycling systems. FNOs catalyze the reduction of NADP⁺ using F₄₂₀H₂ and have been found in a number of archaea (6–10) and bacteria (11) (Fig. 1). It has been argued that in methanogens, FNO catalyzes mainly the reduction of NADP⁺ using F₄₂₀H₂ while bacterial FNOs are supposed to catalyze the reverse reaction (11).

Thermobifida fusca is a moderately thermophilic soil bacterium with high G+C content. This actinomycete holds high biocatalytic potential as it has already served as a source for several highly thermostable enzymes, e.g., catalase, Baeyer–Villiger monooxygenase, and glycoside hydrolases (12–14). Interestingly, a recent bioinformatic study predicted that the *T. fusca* genome contains 16 genes encoding for F₄₂₀-dependent enzymes (15). Nevertheless, there has been so far no biochemical evidence for such enzymes. Here, we describe the identification and characterization of a dimeric thermostable F₄₂₀:NADPH oxidoreductase from *T. fusca* (Tfu-FNO), confirming the presence of F₄₂₀-dependent enzymes in this mesophilic bacterium. Despite the high GC content (67%) of the gene sequence, Tfu-FNO is readily expressed in *E. coli*. Notably, Tfu-FNO is a thermostable enzyme and shows a clear substrate preference towards NADP(H) instead of NAD(H). By solving the three-dimensional crystal structure of Tfu-FNO, we set out site-directed mutagenesis to corroborate the role of residues that interact with the phosphate moiety at 2' position of NADP⁺.

Results

Purification of Tfu-FNO

A BLAST search for Af-FNO homologs in *T. fusca* resulted in the identification of the Tfu_0907 gene (TFU_RS04835). The encoded protein shares 40% and 70% sequence identity to FNOs from *A. fulgidus* and *S. griseus*, respectively (Fig. 2). The Tfu-fno gene, with a high GC content (67%), was amplified from the genomic DNA of *T. fusca* and transformed into *E. coli* TOP10 as a pBAD-fno construct. Purification of the respective protein, Tfu-FNO, was achieved through ammonium sulfate precipitation followed by anion exchange chromatography. DNase I treatment during the first steps of protein purification was found to be essential to remove residual DNA. Tfu-FNO was obtained in pure form with a relatively high yield: 120–200 mg/L culture. It is worth noting that the amount of purified Tfu-FNO obtained in our system is significantly higher than that of Af-FNO when heterologously expressed in *E. coli* [2 mg/L culture (16)].

Effects of pH and temperature on activity

FNOs are known to catalyze the reduction of NADP⁺ at higher pH, while at lower pH it catalyzes the reverse reaction. Figure 3 shows the effect of pH on Tfu-FNO activity. The reduction rate of NADP⁺ is highest at pH 8.5–9.0 while the reverse reaction is optimal between pH 4.0–6.0. From the *k*_{obs} values of both the forward and backward reactions, it can be concluded that FNO catalyzes NADP⁺ reduction more efficiently (Fig. 3). This is in line with the redox potential of F₄₂₀ (–340 mV) being lower when compared with that of NADP⁺ (–320 mV) (3).

Since FNO originates from the mesophilic organism *T. fusca*, the enzyme is expected to be stable at relatively high temperatures. Measuring the activities at temperatures between 25 and 90 °C revealed that the enzyme displays highest activity between 60–70 °C (Fig. 4). The activity at 65 °C is almost 4-time higher than that at 25 °C. The apparent melting temperature of Tfu-FNO was found to be 75 °C, as measured by the Thermofluor® method (17). All the generated Tfu-FNO mutants had melting temperatures similar to the wild-type enzyme (data not shown). This indicates that FNO is remarkably thermostable and is most active at elevated temperatures.

Steady-state kinetics

The steady-state kinetic parameters were measured for NADPH and F₄₂₀ as substrates by following absorbance of these two cofactors at either 340 nm or 400 nm, respectively. The concentration of one substrate was varied while keeping the other substrate at a constant, saturated concentration. The kinetic data fitted well to the Michaelis–Menten kinetic model when the observed rates (k_{obs}) were plotted against substrate concentrations. Tfu-FNO has a K_m value of 7.3 μM and 2.0 μM for NADPH and F₄₂₀, respectively at pH 6.0 and 25 °C (Table 1). Thus, Tfu-FNO has a significantly lower K_m for NADPH (2.0 μM) compared to the values featured by Af-FNO (40 μM) and FNO from *S. griseus* (19.5 μM) (8,11). The k_{cat} (3.3 s⁻¹) of Tfu-FNO is somewhat lower when compared with that of Af-FNO (5.27 s⁻¹) (18).

The overall structure of Tfu-FNO

Crystallization of Tfu-FNO was successful which allowed the elucidation of its crystal structure. This revealed that NADP⁺ had been co-purified with the native enzyme as it was found to be bound in the active site (Fig. 5–6). All crystal soaking attempts to obtain the F₄₂₀ cofactor bound in the enzyme active site failed, which can be explained by the tight molecular packing found in Tfu-FNO crystals that would hamper cofactor binding in the same position as found in Af-FNO (Fig. 5A). It is known that, depending on the bacterial species, the number of glutamate moieties of F₄₂₀ can vary from two to nine, with five to six being the predominant species in mycobacteria (19). Given the crystal arrangement of Tfu-FNO molecules, an oligoglutamate tail of F₄₂₀ of any length would clash against another subunit interacting through crystal packing (Fig. 5A). Nevertheless, the architecture of the active site is highly conserved, and NADP⁺ adopts a virtually identical position with respect to that observed in Af-FNO (Fig. 5B). Therefore, F₄₂₀ was tentatively modelled in Tfu-FNO upon superposition of the archaeal enzyme (Fig. 5C). The modelled F₄₂₀ fits very well into the Tfu-FNO active site without any clashes. Similarly to Af-FNO, F₄₂₀ would bind in Tfu-FNO at the C-terminal domain with its deazaisoalloxazine ring burying deep inside the catalytic pocket and the highly polar oligoglutamyl tail directed towards the exterior of the dimer (Fig. 5B,C).

As mentioned above, NADP⁺ binds to the N-terminal part of Tfu-FNO in a highly similar manner to that of Af-FNO which is characteristic for members of the dinucleotide binding protein family (20,21). The hydrogen bonding network between NADP⁺ and the residues that form the active site are illustrated in Fig. 6. In particular, the nicotinamide ring directly docks to the protein by hydrogen bonding the cofactor amide group to the peptide nitrogen of Ala155 (corresponding to Ala137 in Af-FNO). This conserved interaction is believed to be crucial in conferring the *trans* conformation of the amide group. With this conformation, the pyridine ring of NADP⁺ is maintained planar which in turn facilitates the hydride transfer between the C4 of the NADP and C5 of F₄₂₀ by shortening the distance of the two atoms (20).

NADP⁺ binding site

The residues involved in binding the ADP moiety are also conserved in Tfu-FNO (Fig. 6). Analogous to Af-FNO, the negatively charged group of the ribose 2'-phosphate interacts with the side chains of Thr28, Ser50, Arg51, and Arg55 (corresponding to Thr9, Ser31, Arg32, and Lys36 in Af-FNO). These residues are highly conserved in other known FNOs (Fig. 2). These residues therefore appear to be crucial for substrate recognition and help to discriminate between NADP⁺ and NAD⁺ (20). To get more insights into the role of these residues, they were mutated into amino acids with different charge and/or size, and tested for the cofactor specificity towards the two nicotinamide cofactors. Table 1 shows the kinetic parameters for both NADH and NADPH as substrate. For wild-type Tfu-FNO, the K_m value for NADH (14 mM) is several orders of magnitude higher than that for NADPH (7.3 μM), clearly confirming that the enzyme prefers NADP(H) over NAD(H). For all mutants, the K_m value for NADPH significantly increased (from 2.6- to >68-fold) compared to that of the wild-type enzyme, which verified the crucial role of these residues in binding NADP(H). Intriguingly, recognition of NADH remained the same or improved in all mutants (Table 3), with a K_m value ranging from 0.23- to 2.3-times of that from the wild-type. Noticeably, R55N and R55S variants have a significantly improved affinity towards NADH. In case of mutant R55N, $K_{m, \text{NADPH}}$ increased more than 100 fold while the $K_{m, \text{NADH}}$ decreased almost 4 fold. The S50E mutant was the best among the tested mutants with a $K_{m, \text{NADH}}$ of almost 5-time lower and a K_m ,

NADPH of approximately 100-fold higher as compared to wild-type Tfu-FNO. Interestingly, the T28A mutant showed an increased activity towards both NADPH and NADH, with a 4-fold increase in catalytic rate ($k_{\text{cat}} = 14 \text{ s}^{-1}$) for NADPH and a 2.8-fold decrease in K_{m} value (5 mM) for NADH when compared with the wild-type enzyme. This resulted in significantly improved $k_{\text{cat}}/K_{\text{m}}$ values for both NADPH and NADH, respectively. Unfortunately, combinations of the mutations did not show significant additive effects (Table 1).

Discussion

F₄₂₀-dependent enzymes are interesting candidates for biotechnological applications (5). Recent studies have suggested a widespread occurrence of such deazaflavin-dependent enzymes in actinobacteria (15). Some specific lineages seem especially rich in F₄₂₀-dependent enzymes, such as *Mycobacterium tuberculosis*. This makes members of this superfamily of deazaflavoproteins potential drug targets due to their absence in the human proteome and the human gut flora. The work of Selengut et al. also predicted the presence of at least 16 F₄₂₀ related genes in *T. fusca*, including all genes required for F₄₂₀ biosynthesis (15). Through our study, we have experimentally confirmed the presence of an F₄₂₀-dependent enzyme in this actinomycete by cloning and characterization of a thermostable F₄₂₀:NADPH oxidoreductase (Tfu-FNO), which catalyzes the reduction of NADP⁺ using reduced F₄₂₀ and the reverse reaction.

The role of FNO in generating reduced F₄₂₀

F₄₂₀ cofactor provides microorganism alternative redox pathways. The deazaflavin cofactor seems especially equipped for reduction reactions as it displays a redox potential which is lower when compared with the nicotinamide cofactor. Two enzymes have been identified in previous studies that serve a role in reducing F₄₂₀—FNO and F₄₂₀-dependent glucose-6-phosphate dehydrogenase (FGD) (4). Using *T. fusca* cell-free extract and heterologously expressed Tfu_1669 (a putative *M. tuberculosis* FGD homolog), we could not detect any FGD activity (unpublished data). This suggests that the *T. fusca* proteome indeed does not include an FGD. In fact, it has been shown before that not all actinomycetes have an FGD (22). Therefore, FNO may be the primary enzyme in actinomycetes for providing the cells with F₄₂₀H₂. Nevertheless, at physiological pH (7.0–8.0, Fig. 3) Tfu-FNO performs reduction of NADP⁺ slightly better than reduction of cofactor

F₄₂₀, which is different from the FNO from *S. griseus* (11) and more similar to the archaeal FNOs (7,8). This can partly be explained by the experimental condition (24 °C) differing from the optimum temperature at which the bacteria grow (55 °C) and the intercellular environment (e.g., cofactor concentrations, salt concentrations). Several lines of evidence suggest that in other actinomycetes, such as *Rhodococcus opacus* and *Nocardioideis simplex*, FNO is also the main source of F₄₂₀H₂. In these bacteria, the *fno* gene was embedded in the same operon with genes encoding for the F₄₂₀H₂-dependent reductases, which are involved in the metabolism of picrate and 2,4-dinitrophenols (23–25). FNO-catalyzed regeneration of F₄₂₀H₂ was also proposed to be crucial for the reductive steps in the biosynthesis of tetracycline by *Streptomyces* (26).

Structure and NADP(H) binding site of Tfu-FNO

FNO is believed to be the only F₄₂₀-dependent enzyme known so far that is conserved between archaea and bacteria (4). Except for a 19 amino acid extension loop at the N-terminus, Tfu-FNO largely shares the overall topology and cofactor binding site with that from *A. fulgidus* (Fig. 2 and 5B). The residues that interact directly with the 2'-phosphate group of NADP(H) are also highly conserved (Fig. 6), and have proven to be essential for binding this cofactor. Upon disrupting the hydrogen bonding network by mutagenesis, all the mutants lost virtually all ability to recognize NADPH (Table 1). Intriguingly, the affinity of these variants towards NADH improved, with the T28A mutant being the best in terms of specificity for NADH (3.3-fold higher $k_{\text{cat}}/K_{\text{m}}$ than that of WT). Yet, an efficient NADH-dependent FNO has still to be engineered. For this, a newly developed tool could be explored which can guide structure-inspired switching of coenzyme specificity (27).

Potential applications in biocatalysis

Tfu-FNO represents a highly attractive candidate for the biocatalytic reduction of F₄₂₀. The enzyme is very thermostable, remains active over a wide range of pH (Fig. 3,4), and can be easily expressed in *E. coli* (120–200 mg/L culture). Tfu-FNO is also a relatively fast enzyme, especially with the T28A mutant displaying a k_{cat} of 14 s^{-1} for NADPH (Table 1). Whereas the majority of current enzymatic F₄₂₀H₂ regeneration protocols employ FGDs (28,29), the cost of the expensive, non-recyclable cosubstrate glucose-6-phosphate remains the main bottleneck for the use of such enzyme in large-scale

applications. Therefore, an F₄₂₀H₂-generating system whose cosubstrate could be recycled, such as T28A TfuFNO would be highly promising. Available, robust NAD(P)H regeneration machineries, such as glucose dehydrogenase or other dehydrogenases, have been thoroughly investigated and widely applied in industry (30). Therefore, by combining Tfu-FNO with an appropriate NAD(P)H recycler, F₄₂₀H₂-reductases can be exploited for biocatalytic purposes.

Experimental procedures

Cloning, expression, and purification of Tfu-FNO

Thermobifida fusca YX was grown at 55 °C in Hägerdahl medium and its genomic DNA was extracted using the GeneElute Bacterial Genomic DNA kit (Sigma–Aldrich). The gene *Tfu-fno* (Tfu_0970, TFU_RS04835) was PCR amplified from genomic DNA of *T. fusca* using the pair of primers listed in Table 2 with the *Nde*I and *Hind*III restriction sites introduced at the 5' and 3' positions of the gene, respectively. The purified PCR product and the pBADN/Myc-HisA vector were digested with the restriction enzymes *Nde*I and *Hind*III, purified, and ligated [vector to insert ratio ca. 1 to 5 (mol/mol)] using T4 DNA ligase (Promega) with quick ligation buffer. The pBADN/Myc-HisA vector is a variant of the commercial pBAD/Myc-HisA (Invitrogen) where the unique *Nco*I site at the translation start is replaced with *Nde*I. The ligation product was transformed into chemically competent *E. coli* TOP10 cells using the heat shock method. Correct transformants were confirmed by sequencing the recombinant plasmid pBAD-*fno*.

Site-directed mutagenesis was carried out by using the pBAD-*fno* vector as template and the QuikChange® mutagenesis method with the corresponding pairs of primers listed in Table 2. The primers (200 nM) were used in a 10 µL reaction mixture. In case of the double mutants, plasmids with a single mutation were used as template. The remaining parent template vector was digested by incubating with *Dpn*I (New England Biolab) at 37 °C for 2 h. *Dpn*I was then inactivated at 80 °C for 10 min and the mutant plasmid was transformed into chemically competent *E. coli* TOP10 cells. Mutations were confirmed by sequencing.

E. coli TOP10 cells with pBAD-*fno* were grown overnight at 37 °C, 130 rpm in a 5 ml lysogenic broth (LB) containing 50 µg/ml ampicillin. This pre-culture was used to inoculate 500 ml of the same medium and grown at 37 °C, 130 rpm. When

the OD₆₀₀ reached 0.4–0.6, the protein expression was induced by addition of 0.02% (w/v) arabinose followed by incubation at 30 °C, 130 rpm for 12 h. Cells were harvested by centrifugation at 6000 × g for 15 min (JLA 10.500 rotor, 4 °C) and resuspended in 10 ml of 50 mM KPi pH 7.0 supplemented with 1 µg/ml of DNase I. Cells were sonicated for 7 min (10 sec on, 15 sec off cycle, 70% amplitude) at 4 °C using a VCX130 Vibra-Cell sonicator (Sonics & Materials, Inc., Newton, USA), and then centrifuged at 15000 × g (JA 17 rotor) for 45 min to obtain the cell-free extract. Tfu-FNO was precipitated by adding 50% saturated ammonium sulfate followed by anion exchange chromatography with a HiTrap™ Q HP 5ml (GE Healthcare) column pre-equilibrated with the same resuspension buffer. Tfu-FNO was eluted by using a linear gradient of 0–1 M NaCl in the same buffer. At around 250 mM NaCl, Tfu-FNO started eluting. Excess salt was removed by using PD-10 desalting column and the protein was stored in 50 mM KPi buffer. (GE Healthcare). Protein concentration was estimated using Bradford assay (30).

Temperature, pH optima, and thermostability of Tfu-FNO

F₄₂₀ was isolated from *Mycobacterium smegmatis* mc² 4517 as previously published protocol (32). F₄₂₀H₂ was prepared by biocatalytic reduction of F₄₂₀ using a recombinant F₄₂₀-dependent glucose-6-phosphate dehydrogenase from *Rhodococcus jostii* RHA1 (29) as previously described (28).

The apparent melting temperature, *T*_m, was determined using the *Thermofluor*® technique (17) with a Bio-Rad C1000 Touch Thermal Cycler (Bio-rad Laboratories, Inc.). The reaction volume was 25 µL, containing 10 µM of enzyme and 5 µL of 5 × SYPRO Orange (Invitrogen). To determine the temperature for optimal activity of Tfu-FNO, the enzyme activity was measured using 1.25 mM NADPH and 20 µM F₄₂₀ in 50 mM KPi pH 6.0 in a 100 µL reaction volume. The cuvette containing the substrates in preheated buffer was heated to the tested temperature (25–90 °C) and the reaction was started by adding 10 nM enzyme. The pH optimum was determined for both the forward and backward reactions of Tfu-FNO. F₄₂₀ depletion at 400 nm ($\epsilon_{400} = 25 \text{ mM}^{-1} \text{ cm}^{-1}$) (33,34) or NADH formation at 340 nm ($\epsilon_{340} = 6.22 \text{ mM}^{-1} \text{ cm}^{-1}$) was followed using a V-660 spectrophotometer from Jasco (IJsselstein, The Netherlands). In this experiment, the reaction (100 µL) contained 250 µM NADPH and 20 µM F₄₂₀ (F₄₂₀ reduction); or 250 µM NADP⁺ and 20 µM

F₄₂₀H₂ (NADP⁺reduction) in 50 mM buffer. Sodium acetate, KPi and Tricine-KOH based buffers were used for pH 4.5–5.5, 6.0–7.5 and 8.0–9.5, respectively.

Steady-state kinetic analyses

To determine the kinetic parameters of the enzyme, initial F₄₂₀ reduction rates were measured using a SynergyMX microplate reader (BioTek) using 96-well F-bottom plates (Greiner Bio-One GmbH) at 25 °C. The reaction was performed in 50 mM KPi pH 6.0 and was started by adding 25–50 nM enzyme in the final volume of 200 µL. The concentration of one of the substrates was kept constant (250 µM for NADPH and 20 µM for F₄₂₀, respectively) while varying the concentration of the other substrate. All the measurements were performed in duplicate. A decrease of absorption either at 400 nm (F₄₂₀ reduction, $\epsilon_{400} = 25.7 \text{ mmol}^{-1} \text{ cm}^{-1}$) or at 340 nm (NADPH oxidation, $\epsilon_{340} = 6.22 \text{ mmol}^{-1} \text{ cm}^{-1}$) was followed to determine the observed rates, k_{obs} (s⁻¹). K_m and k_{cat} values for NADP⁺, NADPH, F₄₂₀ and F₄₂₀H₂ were calculated by fitting the data into the Michaelis–Menten kinetic model using nonlinear regression with GraphPad Prism 6.00 (GraphPad Software, La Jolla, CA, USA).

Crystallization, X-ray data collection, and structure determination of Tfu-FNO

Native Tfu-FNO was crystallized using the sitting-drop vapour diffusion technique at 20 °C by mixing equal volumes of 9.0 mg/mL protein in 10 mM Tris/HCl pH 7.5, 100 mM NaCl and of the reservoir solution containing 5% (w/v) PEG 3000, 30% (v/v) PEG 400, 10% (v/v) glycerol, 0.1 M HEPES pH 7.5. Prior to data collection, crystals were cryo-protected in the mother liquor and flash-cooled by plunging them into liquid nitrogen. X-ray diffraction data to 1.8 Å were collected at the ID30B beamline of the European Synchrotron Radiation Facility in Grenoble, France (ESRF). Image indexing, integration, and data scaling were processed with XDS package (35,36) and programs of the CCP4 suite (37). The Tfu-FNO structure was initially solved by molecular replacement method with Phaser (38) using the coordinates of FNO from *A. fulgidus* [PDB ID code 1JAY (20)] which shares 40% sequence identity with Tfu-FNO as a starting model devoid of all ligands and water molecules. Manual model correction and structure analysis was carried out with Coot (39) whereas alternating cycles of refinement was performed with Refmac5

(40). Figures were generated by using UCSF Chimera (41). Atomic coordinates and structure factors were deposited in the Protein Data Bank under the accession code 5N2I. Detailed data processing and refinement statistics are available in Table 3.

Acknowledgements

This work was supported by an Erasmus Mundus action 2 “Svaagata” program from the European Commission via a PhD scholarship provided to HK and a Ubbo Emmius scholarship from the University of Groningen, the Netherlands, awarded to QTN. We thank the European Synchrotron Radiation Facility (ESRF) for providing beamtime and assistance. We are grateful to Dr. G. Bashiri at the Structural Biology Laboratory, School of Biological Sciences and Maurice Wilkins Centre for Molecular Biodiscovery, the University of Auckland, New Zealand for generously providing a culture of *M. smegmatis* mc² 4517 and the plasmid pYUBDuet-FbiABC. A. Giusti, S. Rovida and F. Forneris are acknowledged for their experimental support.

Conflict of interest

The authors declare that they have no conflicts of interest with the contents of this article.

Author contributions

HK and MWF conceived the study and designed the experiments. HK performed the cloning, expression, purification, and biochemical characterization of the Tfu-FNO wild-type and variants. QTN performed the crystallization and solved the structure of Tfu-FNO. AM and CB supervised this part of the study. HK and QTN drafted the manuscript. All authors contributed to analyzing the data and writing the paper.

References

1. Cheeseman, P., Toms–Wood, A., and Wolfe, R.S. (1972) Isolation and properties of a fluorescent compound, factor 420, from *Methanobacterium* strain M.o.H. *J. Bacteriol.* **112**, 527–531
2. Daniels, L., Bakhiet, N., and Harmon, K. (1985) Wide-spread distribution of a 5-deazaflavin cofactor in *Actinomyces* and related bacteria. *Syst. Appl. Microbiol.* **6**, 12–17
3. Jacobson, F., and Walsh, C. (1984) Properties of 7,8-dide-methyl-8-hydroxy-5-deazaflavins relevant to redox coenzyme function in methanogen metabolism. *Biochemistry (N.Y.)* **23**, 979–988

4. Greening, C., Ahmed, F.H., Mohamed, A.E., Lee, B.M., Pandey, G., Warden, A.C., Scott, C., Oakeshott, J.G., Taylor, M.C., and Jackson, C.J. (2016) Physiology, biochemistry, and applications of F₄₂₀- and F_o-dependent redox reactions. *Microbiol. Mol. Biol. Rev.* **80**, 451–493
5. Taylor, M., Scott, C., and Grogan, G. (2013) F₄₂₀-dependent enzymes—potential for applications in biotechnology. *Trends Biotechnol.* **31**, 63–64
6. Eirich, L.D., and Dugger, R.S. (1984) Purification and properties of an F₄₂₀-dependent NADP reductase from *Methanobacterium thermoautotrophicum*. *Biochim. Biophys. Acta (BBA)—General Subjects.* **802**, 454–458
7. de Wit, L., and Eker, A. (1987) 8-Hydroxy-5-deazaflavin-dependent electron transfer in the extreme halophile *Halo bacterium cutirubrum*. *FEMS Microbiol. Lett.* **48**, 121–125
8. Kunow, J., Schwörer, B., Stetter, K.O., and Thauer, R.K. (1993) A F₄₂₀-dependent NADP reductase in the extremely thermophilic sulfate-reducing *Archaeoglobus fulgidus*. *Arch. Microbiol.* **160**, 199–205
9. Berk, H., and Thauer, R.K. (1997) Function of coenzyme F₄₂₀-dependent NADP reductase in methanogenic archaea containing an NADP-dependent alcohol dehydrogenase. *Arch. Microbiol.* **168**, 396–402
10. Elias, D.A., Juck, D.F., Berry, K.A., and Sparling, R. (2000) Purification of the NADP⁺:F₄₂₀ oxidoreductase of *Methanospiraeta stadtmanae*. *Can. J. Microbiol.* **46**, 998–1003
11. Eker, A., Hessels, J., and Meerwaldt, R. (1989) Characterization of an 8-hydroxy-5-deazaflavin: NADPH oxidoreductase from *Streptomyces griseus*. *Biochim. Biophys. Acta (BBA)—General Subjects.* **990**, 80–86
12. Wilson, D.B. (2004) Studies of *Thermobifida fusca* plant cell wall degrading enzymes. *Chem. Rec.* **4**, 72–82
13. Fraaije, M.W., Wu, J., Heuts, D.P., van Hellemond, E.W., Spelberg, J.H.L., and Janssen, D.B. (2005) Discovery of a thermostable Baeyer–Villiger monooxygenase by genome mining. *Appl. Microbiol. Biotechnol.* **66**, 393–400
14. Lončar, N., and Fraaije, M.W. (2015) Not so monofunctional—a case of thermostable *Thermobifida fusca* catalase with peroxidase activity. *Appl. Microbiol. Biotechnol.* **99**, 2225–2232
15. Selengut, J.D., and Haft, D.H. (2010) Unexpected abundance of coenzyme F₄₂₀-dependent enzymes in *Mycobacterium tuberculosis* and other actinobacteria. *J. Bacteriol.* **192**, 5788–5798
16. Le, C.Q., Joseph, E., Nguyen, T., and Johnson-Winters, K. (2015) Optimization of expression and purification of recombinant *Archeoglobus fulgidus* F₄₂₀H₂:NADP⁺ oxidoreductase, an F₄₂₀ cofactor dependent enzyme. *Protein J.* **34**, 391–397
17. Pantoliano, M.W., Petrella, E.C., Kwasnoski, J.D., Lobanov, V.S., Myslik, J., Graf, E., Carver, T., Asel, E., Springer, B.A., Lane, P., and Salemme, F.R. (2001) High-density miniaturized thermal shift assays as a general strategy for drug discovery. *J. Biomol. Screen.* **6**, 429–440
18. Hossain, M.S., Le, C.Q., Joseph, E., Nguyen, T.Q., Johnson-Winters, K., and Foss, F.W. (2015) Convenient synthesis of deazaflavin cofactor FO and its activity in F₄₂₀-dependent NADP reductase. *Org. Biomol. Chem.* **13**, 5082–5085
19. Bair, T.B., Isabelle, D.W., and Daniels, L. (2001) Structures of coenzyme F₄₂₀ in *Mycobacterium* species. *Arch. Microbiol.* **176**, 37–43
20. Warkentin, E., Mamat, B., Sordel-Klippert, M., Wicke, M., Thauer, R.K., Iwata, M., Iwata, S., Ermiler, U., and Shima, S. (2001) Structures of F₄₂₀H₂:NADP⁺ oxidoreductase with and without its substrates bound. *EMBO J.* **20**, 6561–6569
21. Carugo, O., and Argos, P. (1997) NADP-dependent enzymes. II: Evolution of the mono- and dinucleotide binding domains. *Proteins: Struct. Funct. Genet.* **28**, 29–40
22. Purwantini, E., Gillis, T.P., and Daniels, L. (1997) Presence of F₄₂₀-dependent glucose-6-phosphate dehydrogenase in *Mycobacterium* and *Nocardia* species, but absence from *Streptomyces* and *Corynebacterium* species and methanogenic archaea. *FEMS Microbiol. Lett.* **146**, 129–134
23. Heiss, G., Hofmann, K.W., Trachtmann, N., Walters, D.M., Rouvière, P., and Knackmuss, H. (2002) *npd* gene functions of *Rhodococcus (opacus) erythropolis* HL PM-1 in the initial steps of 2,4,6-trinitrophenol degradation. *Microbiology.* **148**, 799–806
24. Ebert, S., Fischer, P., and Knackmuss, H. (2001) Converging catabolism of 2,4,6-trinitrophenol (picric acid) and 2,4-dinitrophenol by *Nocardioides simplex* FJ2-1A. *Biodegradation.* **12**, 367–376
25. Ebert, S., Rieger, P.G., and Knackmuss, H.J. (1999) Function of coenzyme F₄₂₀ in aerobic catabolism of 2,4,6-trinitrophenol and 2,4-dinitrophenol by *Nocardioides simplex* FJ2-1A. *J. Bacteriol.* **181**, 2669–2674
26. Novotná, J., Neužil, J., and Hošťálek, Z. (1989) Spectrophotometric identification of 8-hydroxy-5-deazaflavin:NADPH oxidoreductase activity in streptomycetes producing tetracyclines. *FEMS Microbiol. Lett.* **59**, 241–245
27. Cahn, J.K., Werlang, C.A., Baumschlager, A., Brinkmann-Chen, S., Mayo, S.L., and Arnold, F.H. (2017) A General Tool for Engineering the NAD/NADP Cofactor Preference of Oxidoreductases. *ACS Synth. Biol.* **6**, 326–333
28. Manjunatha, U.H., Boshoff, H., Dowd, C.S., Zhang, L., Albert, T.J., Norton, J.E., Daniels, L., Dick, T., Pang, S.S., and Barry, C.E., 3rd (2006) Identification of a nitroimidazo-oxazine-specific protein involved in PA-824 resistance in *Mycobacterium tuberculosis*. *Proc. Natl. Acad. Sci. U.S.A.* **103**, 431–436
29. Nguyen, Q.-T., Trinco, G., Binda, C., Mattevi, A., and Fraaije, M.W. (2016) Discovery and characterization of an F₄₂₀-dependent glucose-6-phosphate dehydrogenase (Rh-FGD1) from *Rhodococcus jostii* RHA1. *Appl. Microbiol. Biotechnol.* 10.1007/s00253-016-8038-y

30. Wichmann, R., and Vasic-Racki, D. (2005) Cofactor regeneration at the lab scale. *Adv. Biochem. Eng. Biotechnol.* **92**, 225–260
31. Bradford, M.M. (1976) A rapid and sensitive method for the quantitation of microgram quantities of protein utilizing the principle of protein–dye binding. *Anal. Biochem.* **72**, 248–254
32. Isabelle, D., Simpson, D.R., and Daniels, L. (2002) Large-scale production of coenzyme F₄₂₀-5,6 by using *Mycobacterium smegmatis*. *Appl. Environ. Microbiol.* **68**, 5750–5755
33. Jacobson, F.S., Daniels, L., Fox, J.A., Walsh, C.T., and Orme-Johnson, W.H. (1982) Purification and properties of an 8-hydroxy-5-deazaflavin-reducing hydrogenase from *Methanobacterium thermoautotrophicum*. *J. Biol. Chem.* **257**, 3385–3388
34. DiMarco, A.A., Bobik, T.A., and Wolfe, R.S. (1990) Unusual coenzymes of methanogenesis. *Annu. Rev. Biochem.* **59**, 355–394
35. Kabsch, W. (2010) Xds. *Acta Crystallographica Section D: Biological Crystallography*. **66**, 125–132
36. Kabsch, W. (2010) Integration, scaling, space-group assignment and post-refinement. *Acta. Crystallogr. Sect. D: Biol. Crystallogr.* **66**, 133–144
37. Winn, M.D., Ballard, C.C., Cowtan, K.D., Dodson, E.J., Emsley, P., Evans, P.R., Keegan, R.M., Krissinel, E.B., Leslie, A.G., McCoy, A., McNicholas, S.J., Murshudov, G.N., Pannu, N.S., Potterton, E.A., Powell, H.R., Read, R.J., Vagin, A., and Wilson, K.S. (2011) Overview of the CCP4 suite and current developments. *Acta Crystallogr. Sect. D: Biol. Crystallogr.* **67**, 235–242
38. McCoy, A.J., Grosse-Kunstleve, R.W., Adams, P.D., Winn, M.D., Storoni, L.C., and Read, R.J. (2007) Phaser crystallographic software. *J. Appl. Crystallogr.* **40**, 658–674
39. Emsley, P., and Cowtan, K. (2004) Coot: model-building tools for molecular graphics. *Acta Crystallogr. Sect. D: Biol. Crystallogr.* **60**, 2126–2132
40. Murshudov, G.N., Vagin, A.A., and Dodson, E.J. (1997) Refinement of macromolecular structures by the maximum-likelihood method. *Acta Crystallogr. Sect. D: Biol. Crystallogr.* **53**, 240–255
41. Pettersen, E.F., Goddard, T.D., Huang, C.C., Couch, G.S., Greenblatt, D.M., Meng, E.C., and Ferrin, T.E. (2004) UCSF Chimera—a visualization system for exploratory research and analysis. *J. Comput. Chem.* **25**, 1605–1612

Table 1 Steady-state kinetic parameters for wild-type and mutant Tfu-FNOs using NADH and NADPH as substrate. n.d., not determined.

Tfu-FNO variant	NADH			NADPH			$k_{\text{cat}}/K_{\text{m, NADPH}}/$ $k_{\text{cat}}/K_{\text{m, NADH}}$
	K_{m} (mM)	k_{cat} (s ⁻¹)	$k_{\text{cat}}/K_{\text{m}}$ (M ⁻¹ s ⁻¹)	K_{m} (μM)	k_{cat} (s ⁻¹)	$k_{\text{cat}}/K_{\text{m}}$ (mM ⁻¹ s ⁻¹)	
Wild-type	14 ± 4.2	2.2 ± 0.4	160	7.3 ± 1.0	3.3 ± 0.1	450	2800
R51A	8.6 ± 0.9	3.2 ± 0.2	370	>180	>1.6	6.2	17
R51V	8.7 ± 1.1	3.4 ± 0.2	290	>180	>1.3	9.3	32
R55A	7.0 ± 0.8	3.0 ± 0.2	420	29 ± 4.0	8.8 ± 0.3	300	710
R55N	6.3 ± 3.6	2.8 ± 0.7	440	>500	n.d.		
R55S	4.4 ± 1.3	3.5 ± 0.4	790	170 ± 38	6.9 ± 0.7	41	52
R55V	9.6 ± 1.4	3.2 ± 0.2	330	49 ± 7.2	n.d.		
S50E	3.2 ± 1.0	2.7 ± 0.3	840	>500	n.d.		
S50Q	8.2 ± 2.7	4.2 ± 0.6	510	>500	n.d.		
T28A	5.0 ± 0.6	2.6 ± 0.1	520	19 ± 2.6	14 ± 0.5	720	1400
R51ER55A	10 ± 2.7	1.6 ± 0.2	160	>500	n.d.		
R51ER55N	6.5 ± 1.3	2.7 ± 0.2	420	>500	n.d.		
R51ER55S	32 ± 1.9	4.9 ± 0.2	150	>500	n.d.		
R51VR55V	10 ± 1.4	2.8 ± 0.2	280	>500	n.d.		
S50ER55A	20 ± 9.2	2.3 ± 0.7	120	>500	n.d.		
S50ER55V	9.8 ± 2.3	1.8 ± 0.2	180	>500	n.d.		
T28AR51V	12 ± 2.2	2.7 ± 0.3	230	>500	n.d.		
T28AR55A	5.4 ± 1.5	2.5 ± 0.3	460	93 ± 29	3.3 ± 0.4	3.5	8
T28AR51VR55V	12 ± 2.2	3.3 ± 0.3	280	>500	n.d.		

Table 2 Primers used in this study. Sites of mutations are marked with oligonucleotides in bold, whereas restriction sites are in bold, italic.

<i>fno</i> genes	Forward primers (5'–3')	Reverse primers (5'–3')
FNO WT	TGCC <i>ATATG</i> TCGATTGCCGTGCTG TCG	<i>AAGCTT</i> TAGATGTCGGTGATGCGGATAC
FNO_R51M	TGATTCTCGGTT CGATG AGCGCGGAGCGGG	CCCGCTCCGCGCT CAT CGAACCGAGAATCA
FNO_S50Q	GCACGAGGTGATTCTCGGT CAG CGGAGCGCG	CGCGCTCCG CTG ACCGAGAATCACCTCGTGC
FNO_S50E	GCACGAGGTGATTCTCGGT GAG CGGAGCGCG	CGCGCTCCG CTC ACCGAGAATCACCTCGTGC
FNO_R55S	GGAGCGCGGAG AGC GCCCAGGCGGT	ACCGCCTGGGCG CTC TCCGCGCTCC
FNO_R55N	GCGGAGCGCGGAG AAC GCCCAGGCGGTTG	CAACCGCCTGGGCG TTT TCTCCGCGCTCCGC
FNO_T28A	GTGCTGGGGGG CGCG GGTGATCAGG	CCTGATCAC CCCG CGCCCCCAGCAC
FNO_R51A	GATTCTCGGTT CGGCG AGCGCGGAGCGG	CCGCTCCGCGCT CGC CGAACCGAGAATC
FNO_R51V	GATTCTCGGTT CGGTG AGCGCGGAGCGG	CCGCTCCGCGCT CAC CGAACCGAGAATC
FNO_R51E	GATTCTCGGTT CGGAG AGCGCGGAGCGG	CCGCTCCGCGCT CTC CGAACCGAGAATC
FNO_R55A	GGAGCGCGGAG GCG GCCCAGGCGG	CCGCCTGGG CCG CCTCCGCGCTCC
FNO_R55V	GGAGCGCGGAG GTG GCCCAGGCGG	CCGCCTGGG CCAC CTCCGCGCTCC
FNO_R55E	GGAGCGCGGAG GAG GCCCAGGCGG	CCGCCTGGG CCCT CCTCCGCGCTCC
FNO_S50A	ACGAGGTGATTCTCGGT GCG CGGAGCG	CGCTCCG CGC ACCGAGAATCACCTCGT

Table 3 Data collection and refinement statistics

PDB ID Code	5N2I
Space group	$P2_12_12_1$
Resolution (Å)	1.80
a, b, c (Å)	82.4, 86.1, 136.8
$R_{\text{sym}}^{\text{a,b}}$ (%)	11.2 (99.1)
Completeness ^b (%)	98.6 (90.2)
Unique reflections	89383
Multiplicity ^b	4.5 (2.8)
I/σ^b	7.9 (0.9)
$CC_{1/2}^b$	99.4 (24.7)
Number of atoms:	
protein	6594
NADP ⁺ /glycerol/water	$4 \times 48/7 \times 6/600$
Average B value for all atoms (Å ²)	25.0
$R_{\text{cryst}}^{\text{b,c}}$ (%)	16.5 (34.1)
$R_{\text{free}}^{\text{b,c}}$ (%)	21.4 (35.7)
Rms bond length (Å)	0.019
Rms bond angles (°)	2.02
Ramachandran outliers	0

^a $R_{\text{sym}} = \sum |I_i - \langle I \rangle| / \sum I_i$, where I_i is the intensity of i^{th} observation and $\langle I \rangle$ is the mean intensity of the reflection.

^b Values in parentheses are for reflections in the highest resolution shell.

^c $R_{\text{cryst}} = \sum |F_{\text{obs}} - F_{\text{calc}}| / \sum |F_{\text{obs}}|$ where F_{obs} and F_{calc} are the observed and calculated structure factor amplitudes, respectively. R_{cryst} and R_{free} were calculated using the working and test sets, respectively.

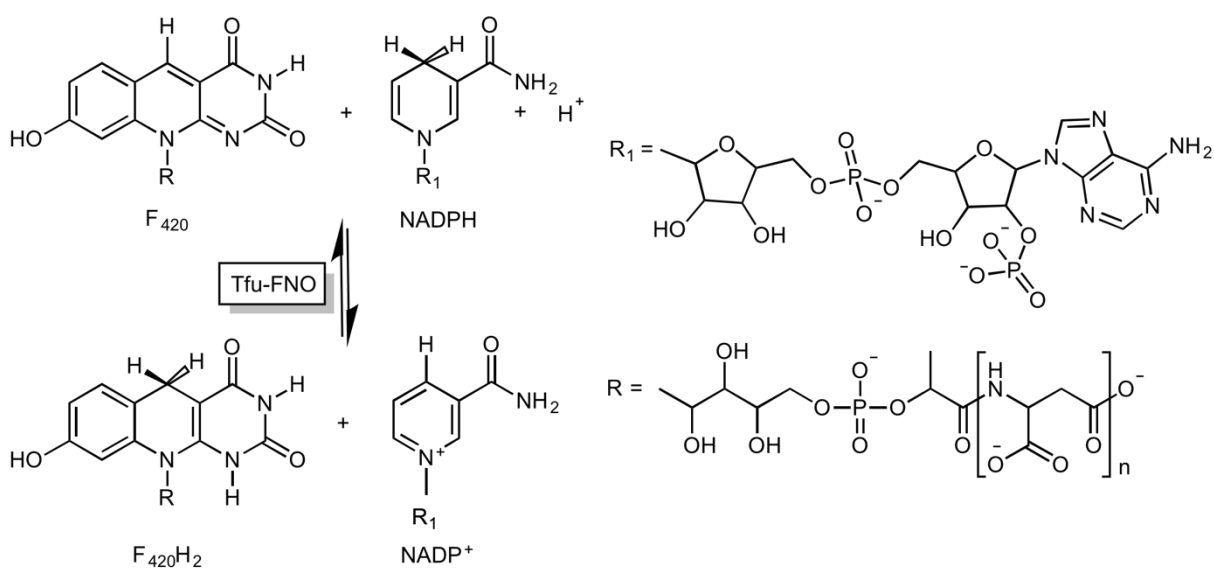


Figure 1 The reversible reaction catalyzed by F₄₂₀:NADPH oxidoreductase. The number of glutamate residues attached to the phospholactyl moiety may vary (n = 2–8 in case of *Mycobacterium smegmatis*).

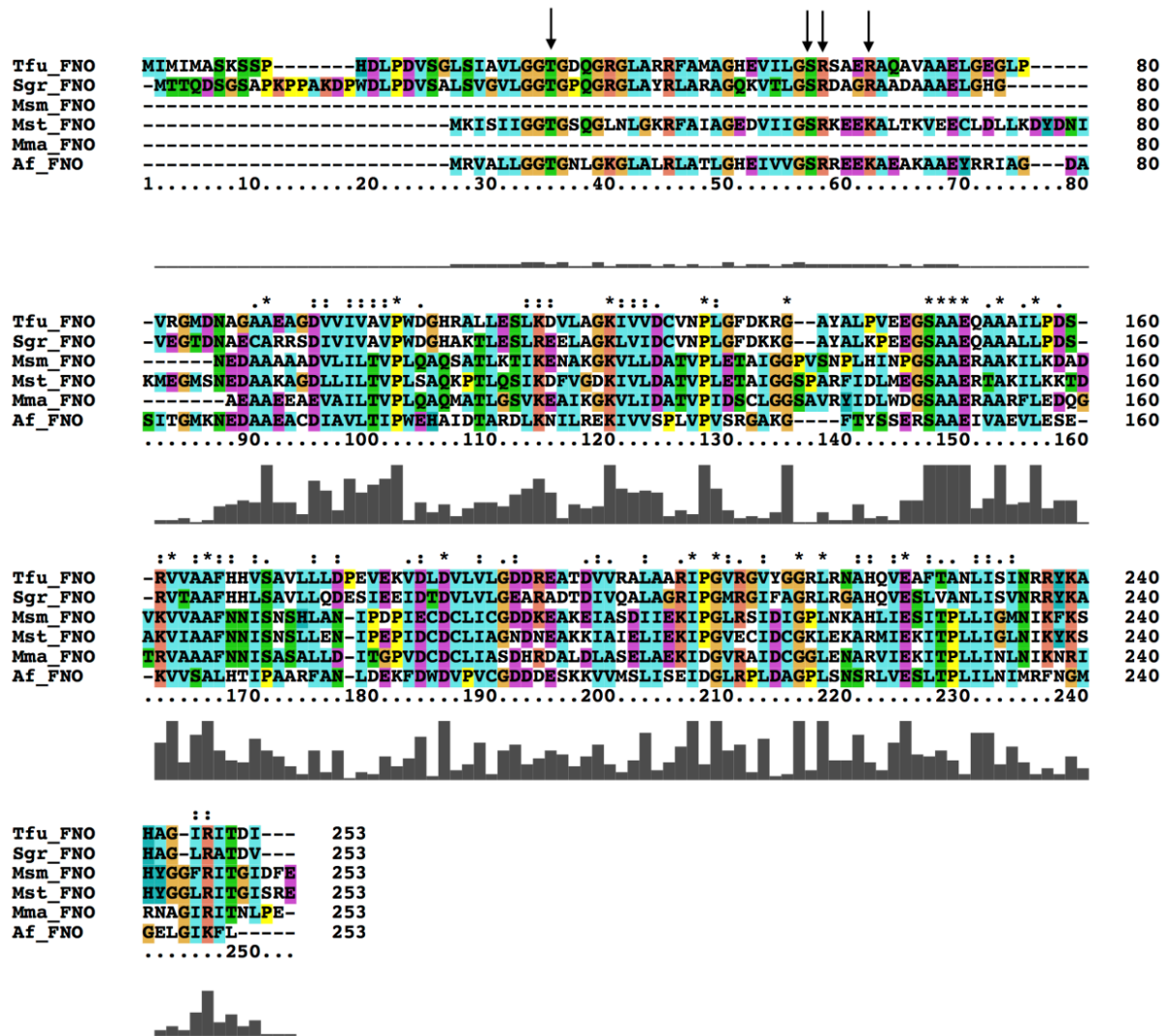


Figure 2 Multiple sequence alignment of selected FNOs from *Thermobifida fusca* (Tfu_FNO), *Archaeoglobus fulgidus* (Af_FNO), *Methanothermobacter marburgensis* (Mma_FNO), *Methanobrevibacter smithii* (Msm_FNO), *Methanosphaera stadtmanae* (Mst_FNO), and *Streptomyces griseus* (Sgr_FNO). The figure was generated with Clustal X2.1. Residues involved in binding the 2'-phosphate group of NADP⁺ are indicated with an arrow.

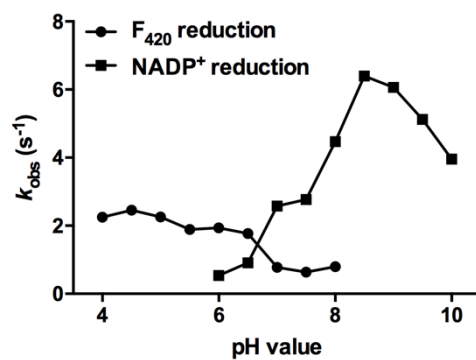


Figure 3 pH optimum for the Tfu-FNO-catalyzed F₄₂₀ reduction using NADPH (dots) or the NADP⁺ reduction using F₄₂₀H₂ (squares) at 24 °C. k_{obs} (s⁻¹) for the NADP⁺ reduction (pH optima 8–10) is almost 3-time higher than that for the F₄₂₀ reduction (pH optimum 4–6).

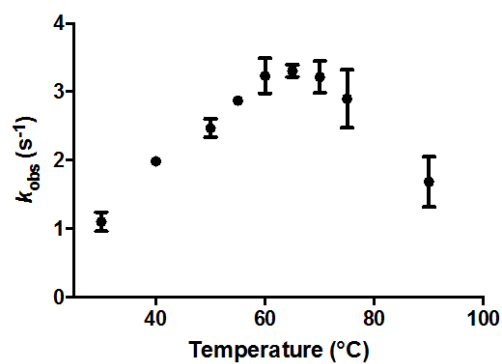
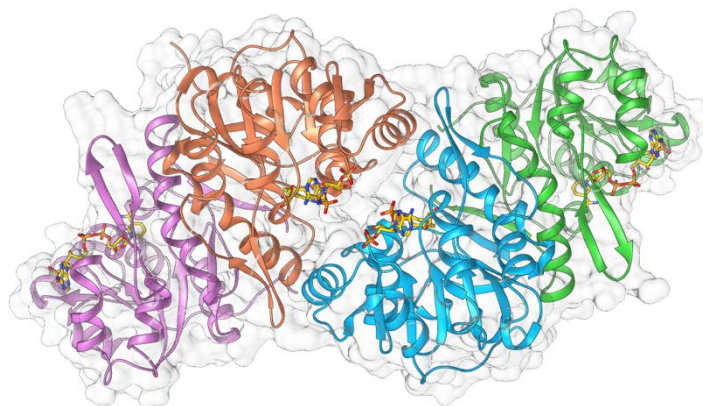
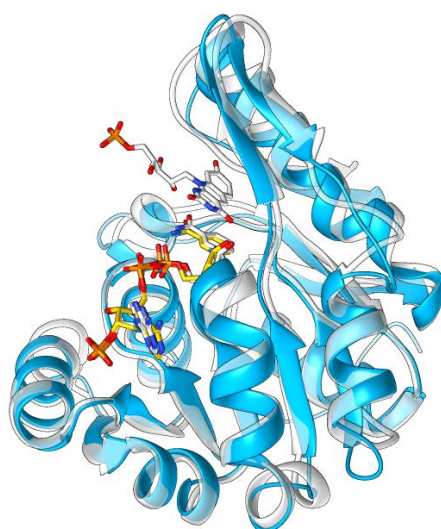


Figure 4 Effect of temperature on Tfu-FNO activity. Reaction mixture of 100 μ L contained 1.25 mM NADH, 20 μ M F_{420} in 50 mM KPi pH 6.0. The reaction was started by adding 50 nM FNO. The error bars represent standard deviation from two measurements.

A



B



C

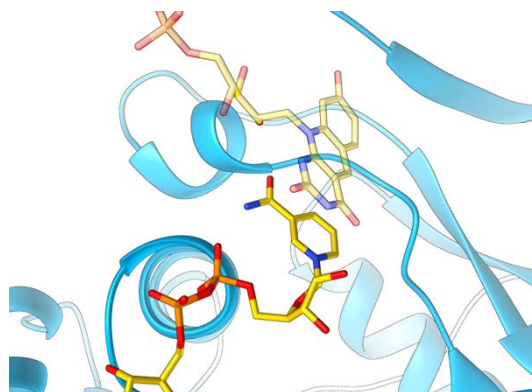


Figure 5 Crystal structure of FNO from *Thermobifida fusca* (A) The asymmetric unit of Tfu-FNO crystals contain two dimers AB and CD, colored in coral (monomer A), orchid (monomer B), deep sky blue (monomer C), and green (monomer D), respectively. (B) Superposition of the Tfu-FNO monomer C onto the homologous NADP⁺- and F₄₂₀-bound Af-FNO monomer [carbon atoms in white, 40% sequence identity, PDB ID 1JAY (20)]. The two structures largely share the same overall topology and the binding pocket architecture, with the nicotinamide rings adopting a similar position in the active site. (C) Close-up view of Tfu-FNO binding pocket with a modelled F₄₂₀ molecule (in

shaded colors with carbon atoms in yellow) as a result of superposition as in **B**. The NADP(H) carbon atoms are shown in yellow, oxygen atoms in red, nitrogen atoms in blue, and phosphorous atoms in orange.

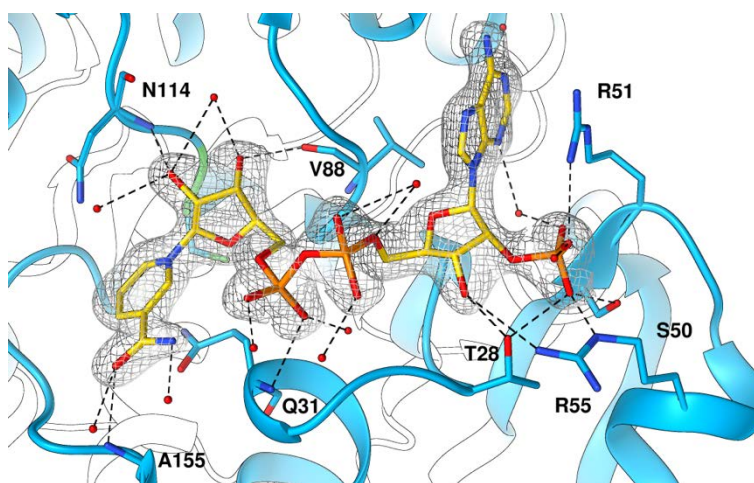


Figure 6 Active site of Tfu-FNO in complex with NADP⁺. Unbiased $2F_o - F_c$ electron density map calculated at 1.8 Å and contoured at 1.0 σ are drawn as grey chicken-wire. Potential hydrogen bonds are depicted with dashed lines and water molecules as red spheres. Residues in direct contact with NADP⁺ are labeled. The orientation of the molecule is approximately 180° clockwise rotated along an axis perpendicular to the plane of the paper with respect to that in Figure 5. Color coding for atoms is as in Figure 5.

**Isolation and characterization of a thermostable F₄₂₀:NADPH oxidoreductase from
*Thermobifida fusca***

Hemant Kumar, Quoc-Thai Nguyen, Claudia Binda, Andrea Mattevi and Marco W. Fraaije
J. Biol. Chem. published online April 14, 2017

Access the most updated version of this article at doi: [10.1074/jbc.M117.787754](https://doi.org/10.1074/jbc.M117.787754)

Alerts:

- [When this article is cited](#)
- [When a correction for this article is posted](#)

[Click here](#) to choose from all of JBC's e-mail alerts

This article cites 0 references, 0 of which can be accessed free at
<http://www.jbc.org/content/early/2017/04/14/jbc.M117.787754.full.html#ref-list-1>